Research & Reviews: Journal of Statistics and Mathematical Sciences

Type-III Intermittency from Markov Binary Block Visibility Graph Perspective

Pejman Bordbar and Sodeif Ahadpour*

University of Mohaghegh Ardabili, Ardabil, Iran

Research Article

Received date: 08/02/2019

Accepted date: 25/02/2019

Published date: 04/03/2019

***For Correspondence**

Faculty of Sciences, University of Mohaghegh Ardabili, Ardabil, Iran.

E-mail: ahadpour@uma.ac.ir

Keywords: Type-III Intermittency, binary block design, Markov binary visibility graph, Chaos

ABSTRACT

In this work, the type-III intermittency is studied from the optimized Markov binary visibility graphs perspective. In fact, we study the behavior of a dynamical system in the vicinity of an inverse period doubling bifurcation using networks language. We find their properties based on statistical tools such as the length between reinjection points and the mean length and also length distributions. Numerical results show that asymptotic mode and new nonlinear term affect the trajectory and the mechanism of type-III intermittency, but the mean length is approximately similar to previous works. For further study, we compute the degree distribution of the complex network generated by type-III intermittency. Experimental results are found to agree well with the analytical results derived from the optimized Markov binary visibility graph and also theoretical degree distribution can distinguish two states $\eta \leq \eta_\delta$ and $\eta > \eta_\delta$ from each other in type-III intermittency mechanism.

INTRODUCTION

Intermittency mechanism transitionally occurs between laminar and chaotic zone as a specific configuration of the ergodic dynamical system. Intermittency concept first was introduced by Pomeau and Manneville when Floquet multipliers of the local Poincaré map associated with the Lorenz system traverses the unit circle [1]. A Lorentz system can show chaotic burst at irregular zones by a small change in a control parameter when is in regular behavior [2]. There are various types of intermittencies such as Type-I, II, III [1], X [3], V [4-6], on-off [7,8], eyelet [9,10], spatiotemporal [11], Crisis-induced [11], and ring [12] have been classified chiefly by the local Poincare map [13]. As we Know, in vicinity a tangent bifurcation, a subcritical Hopf bifurcation and an inverse period doubling bifurcation occur Type-I, II, III intermittency when the Floquet multiplier for the local Poincaré map traverses the circle of unitary norm in the complex plane through +1, two complex eigenvalues of Floquet matrix cross the unitary circle off the real axis, and Floquet multiplier is 1, respectively [14]. Type-III intermittency appears in phenomenological processes such as electronic nonlinear devices, lasers, biological tissues and etc [15-18]. Describing the dynamics of intermittency using networks language is our aim in this work. Here, we focus on the study of type-III intermittency based on the complex network extracted from time series of the type-III intermittency. The Markov binary visibility graph is a complex network which is designed based on a Markov chain. It can be optimized by binary block design method to study of behavior and phases of the type-III intermittency which can call it Markov Binary Block Visibility Graph (MBBVG) [19,20]. In the other words, we transform fluctuations of the time series of type-III intermittency into two-state Markov chain using binary block design and then based on the Markov binary visibility graph, the MBBVG map the two-state Markov chain into complex networks. The binary block design is a subcategory of the block design in combinatorial mathematics which has many applications in sciences such as experimental design [21,22], finite geometry [23], software testing [24], cryptography [25,26], and algebraic geometry [27]. Results of the MBBVG will show the capability of it for analyzing the fluctuated properties of the type-III intermittency. This paper is ordered as we study the fluctuated properties of Type-III intermittency in section 2. Then, we study the binary block design in order to use in the construction of the Markov binary visibility graph in section 3. Next, we illustrate the perspective of Markov binary visibility graph that can be used to fluctuation analysis of type-III intermittency in section 4 and finally, in Section 5, we conclude this work.

TYPE-III INTERMITTENCY

The first time, Type-III intermittency was discussed by Pomeau and Manneville [1] in association with the Lorenz model and was observed by Dubois [28] in the Bénard convection of a rectangular cell. For simulation of type-III intermittency by a one dimensional local Poincare map $g(x)$, the Schwartzian derivative $Sg(x)$ must be positive at the critical point [29], that is

$$Sg(x)=\frac{g'''(x)}{g'(x)}-1.5\left(\frac{g''(x)}{g'(x)}\right)^2>0 \tag{1}$$

Here, we propose a local Poincare map with the positive Schwartzian derivative for the illustrative model such

$$U_{n+1}(x)=-(1+\dot{o})U_n(x)-\lambda U_n^3(x)+\eta\frac{U_n^z(x)}{U_n^{'}(x)} \tag{2}$$

that we consider λ>0, z=15 and *U(x)* as a self-map such as a *sin(x)* so that the system is unstable for 0<ϵ≪1 in *x*=0. Also, equation (2) can be simplified to

$$U_{n+1}(x)\approx-(1+\dot{o})U_n(x)-\lambda U_n^3(x) \tag{3}$$

in the vicinity *x=0* as a local Poincare map for type-III intermittency systems [30]. The non-linear term $\eta\frac{U_n^z(x)}{U_n^{'}(x)}$ allows a different reinjection mechanism to be investigated in type-III intermittency. In our simulation, use of a self-map such as a *sin(x)* in the structure of the proposed local Poincare map allows an efficient reinjection mechanism to occur in the intermittency. To consider ϵ=10^{-2} and *sin(x)* as the self-map, extremum points in the exponential trajectory of the map are as x_m= ± 1.0582.

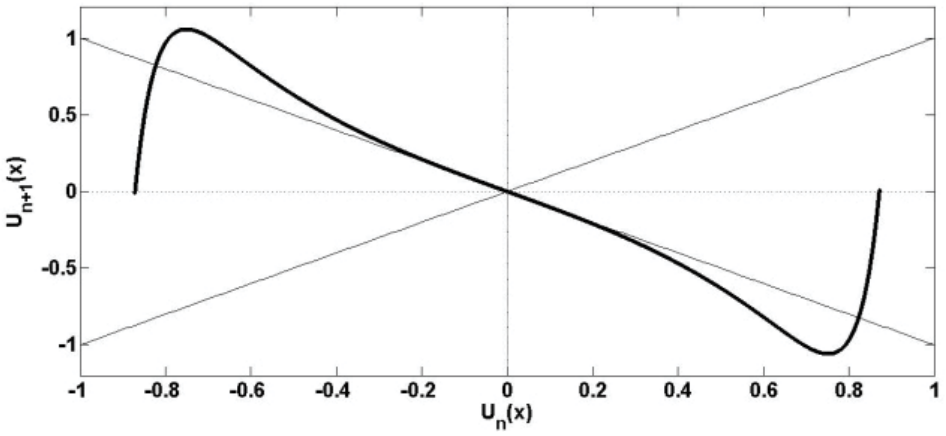

Figure 1. The one-iterated map of the equation (2) based on $U_n(x)$ with control parameters ϵ=10^{-2}, λ=1, and η=6.3.

Figure 1 shows the extremum points of the map that affect the reinjection mechanism. The behavior of the periodic-exponential trajectories is typically as laminar with a long length of n iterations in between reinjected points (x_0=*0*) close to the unstable fixed point **(Figure 2)**. If the rejected points (x_0≪*1*) are far from the unstable fixed point, the behavior of the periodic-exponential trajectories is chaotic burst as short laminar with the length of n iterations.

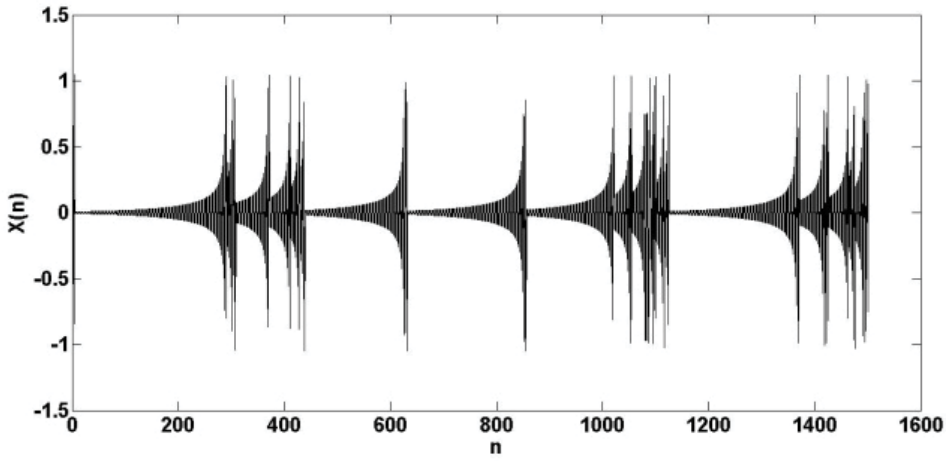

Figure 2. The periodic-exponential trajectories of equation (2) for ϵ=10^{-2}, λ=1, and η=6 based on *n* iterations.

To consider ϵ=10^{-2} and λ=1, the bifurcation diagram of the map (2) shows that no reinjection emerges nearby the fixed point for η>$\eta_\delta \simeq 6.32$ **(Figure 3)**.

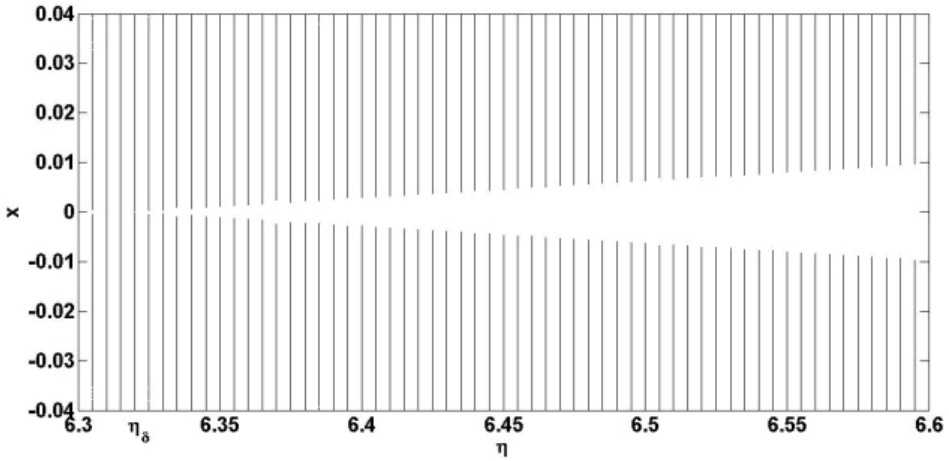

Figure 3. Bifurcation diagram for the equation (2) with $\epsilon=10^{-2}$ and $\lambda=1$.

We focus on the study of the property of type-III intermittency systems. The average laminar length of laminar zones is one of the characteristic relations of type-III intermittency which is typically proportional to the inverse of the value of the distance between the dynamical system and inverse period doubling bifurcation, i.e. $\langle l \rangle \propto \epsilon^{-1}$. To investigate the topic, the equation (2) with $\lambda=1$ can be approximated in the laminar zone by the following differential equation

$$\frac{d|x|}{dn} = U(|x|)\left(\dot{o} + U^2(|x|)\right) \tag{4}$$

that the number of interactions between reinjections (n) is computed as follows

$$\int_{|x|}^{\delta} \frac{dz}{U(z)\left(\dot{o} + U^2(z)\right)} = \int_0^n dn \tag{5}$$

where the δ is the upper limit for the laminar region. In result, the equation of the n is as following

$$n(|x|) = \frac{\dot{o}^{-1}}{2}\left[2\ln\frac{\sin(a\delta)}{\sin(a|x|)} - \ln\frac{\left(\dot{o} + sin^2(a\delta)\right)}{\left(\dot{o} + sin^2(ax)\right)}\right] \tag{6}$$

where a can be equal to 0.87.

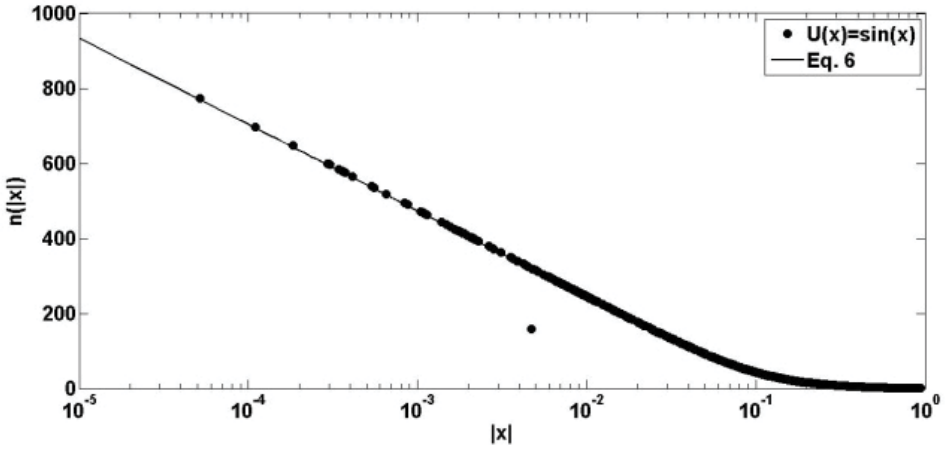

Figure 4. A semi-log plot of a number of interactions between reinjections (solid circles) for the approximation of the equation (2) with $\epsilon=10^{-2}$ and the trajectory of length $N=10^6$. The lines are theoretical predictions based on relations of Equation (6).

As we know, the reinjection probability density (RPD) $\psi(|x|)$ determines the statistical behavior of the intermittency phenomenon [31]. Because the RPD cannot be simply measured by the numerical data, we can use from centroid equation of the RPD in order to compute the RPD which is as following

$$M(x) = \frac{\int_0^x \tau\psi(\tau)d\tau}{\int_0^x \psi(\tau)d\tau} \quad if \int_0^x \psi(\tau)d\tau \neq 0 \tag{7}$$

here, x∈[0,δ] and the δ is the upper bound for the local regular [32]. If we consider the lower bound of the reinjection is slightly greater than zero (x_i>0 and $x_i \approx 0$), the *M(x)* can be numerically approximated in a linear form as [32]

$$M(x) = mx + x_i \tag{8}$$

In result, the RPD can be obtained as follows [33]

$$\psi(x) = b(x - x_i)^{\kappa} \quad with\, \kappa = \frac{1-2m}{m-1} \tag{9}$$

The b with regard to the symmetric property of the RPD is determined by the normalization condition as

$$\int_0^{\delta} 2b(x - x_i)^{\kappa}\, dx = 1 \tag{10}$$

that to consider κ>-1 (0<m<1), the equation (10) is solvable and the b is as [32]:

$$b = \frac{\kappa+1}{2(\delta - x_i)^{\kappa+1}} = \frac{m}{2(1-m)}(\delta - x_i)^{\frac{m}{m-1}} \tag{11}$$

Now, if we consider the lower bound of the reinjection is slightly smaller than zero (x_i<0 and $x_i \approx 0$) and due to the symmetry of the equation, the RPD must be also symmetric [30]. The RPD can be obtained by two overlapping functions, each one having the form given by equation (8) as follows [30]

$$\psi(x) = \begin{cases} b\left[(|x_i| + x)^{\kappa} + (|x_i| - x)^{\kappa}\right] & |x| \le |x_i| \\ b(|x_i| + x)^{\kappa} & |x_i| < x \le \delta \\ b(|x_i| - x)^{\kappa} & -\delta < x \le -|x_i| \end{cases} \tag{12}$$

The b is again determined by the normalization condition and as follows

$$2b\left[\int_0^{|x_i|} (|x_i| + x)^{\kappa} + (|x_i| - x)^{\kappa}\, dx + \int_{|x_i|}^{\delta} (|x_i| + x)^{\kappa}\, dx\right] = 1 \tag{13}$$

that to consider κ>-1, the b is as

$$b = \frac{\kappa+1}{2(\delta - |x_i|)^{\kappa+1}} = \frac{m}{2(1-m)}(\delta - |x_i|)^{\frac{m}{m-1}} \tag{14}$$

In result, it can be obtained as [30]

$$M(x) = \begin{cases} (1-m)\left(\frac{m}{1-m}x - |x_i| + 2\frac{|x_i|(|x_i| - x)^{\frac{m}{1-m}} - |x_i|^{\frac{1}{1-m}}}{(|x_i| - x)^{\frac{m}{1-m}} - (|x_i| + x)^{\frac{m}{1-m}}}\right) & 0 < x < |x_i| \\ \left(2m - 1 + (1-m)2^{\frac{1-2m}{1-m}}\right)|x_i| & x = |x_i| \end{cases} \tag{15}$$

A duration probability density of the local regular φ(n) is related to the RPD and because of the symmetry of the equation (2), it can be as ψ(|x|)=2ψ(x) for x>0 [30,33] then,

$$\varphi(n) = 2\psi(X(n))\left|\frac{dX(n)}{dn}\right| \tag{16}$$

where the function *X(n)* is the inverse function of *n(X)* and for relations of equation (6) is as following

$$X(n)=\mathrm{a}^{-1}\sin^{-1}\left(\sqrt{\frac{\varepsilon}{e^{2\delta n}\left(1+\frac{\delta}{\sin^2(a\delta)}\right)-1}}\right) \tag{17}$$

Numerical results obtained from equation (2) with $\epsilon=10^{-2}$ show the reinjection is periodically uniform in interval (0,δ] so that the interval can be divided into distinct intervals as $(0,|x_i|)$ and $[|x_i|,\delta]$ that values of the m are approximately equal to 0.5 and 0.43, respectively. Also, the values of the x_i and the δ are equal to 0.0117 and 0.9375, respectively **(Figure 5)**.

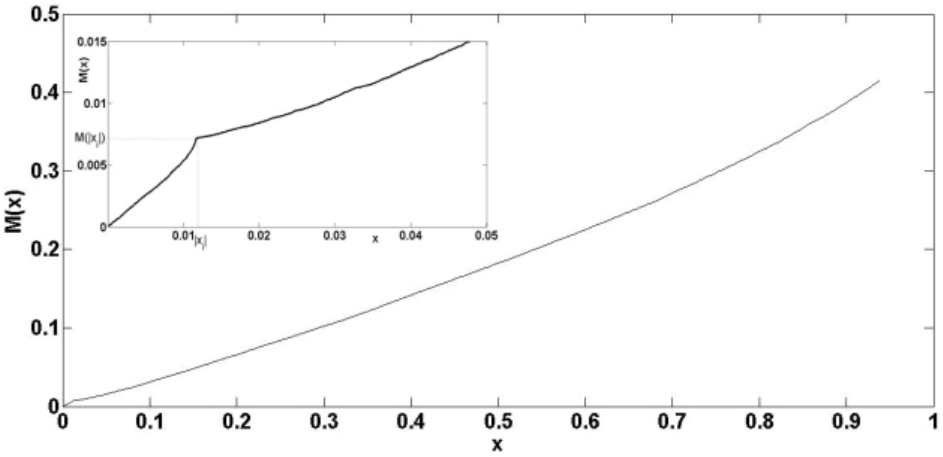

Figure 5. A numerical simulations plot of the centroid equation of the RPD of versus rejected points for equation (2) with $\epsilon=10^{-2}$ and the trajectory of length $N=10^6$. (Insert upper panel) The part of the plot which is located between 0 and 0.05.

The RPD can be obtained for $\epsilon=10^{-2}$as follows

$$\psi\left(X(n)\right)=\begin{cases}\psi_1=0.54r & |x|\le|x_i|\\ \psi_2=0.69\left(0.0117+X(n)\right)^{0.25} & |x_i|<x\le\delta\\ \psi_3=0.69\left(0.0117-X(n)\right)^{0.25} & -\delta<x\le-|x_i|\end{cases} \tag{18}$$

where r is an approximation coefficient. According to the above mention and equation (16), we can obtain the duration probability density *φ(n)* as following **(Figure 6)**

$$\varphi(n)=\left(\psi_1+\psi_2\left(X(n)\right)+\psi_3\left(X(n)\right)\right)\frac{2\delta^{\frac{3}{2}}}{a}\frac{\rho e^{2\delta n}\left(\rho e^{2\delta n}-1\right)^{-\frac{3}{2}}}{\sqrt{1-\delta\left(\rho e^{2\delta n}-1\right)^{-1}}} \tag{19}$$

where ρ is equal to $\left(1+\frac{\delta}{\sin^2(a\delta)}\right)$. Note that we can approximate behaviors of the duration probability density φ(n) based on a characteristic iteration scale n_m [34] in little iterations $n\ll n_m$ and much iterations $n\gg n_m$. For equation (19), we obtain a quadratic behavior in little iterations and an exponential behavior in many iterations as

$$\varphi(n)\approx\begin{cases}\rho\delta^{\frac{1}{2}}\left(n^2-n+4\right), & n\ll n_m\\ 8\rho^4\delta^{\frac{3}{2}}e^{-\delta n}, & n\gg n_m\end{cases} \tag{20}$$

Now, we can compute the average number of interactions ⟨*n*⟩ as characteristic relations based on the above equations using the following equation [34]

$$n=\int_{n_0}^{\infty}n\varphi(n)dn,\quad n_0\cong 0 \tag{21}$$

We obtain the average number of iterations ⟨n⟩ as

$$n \approx \rho\delta^{-\frac{1}{2}}\int_{n_0}^{n_m} n\left(n^2-n+4\right)dn + 8\rho^4\delta^{-\frac{3}{2}}\int_{n_m}^{\infty} ne^{-\delta n}dn = \rho\left(\frac{n_m^4}{4}-\frac{n_m^3}{3}+4n_m\right)\delta^{-\frac{1}{2}} + 8\rho^4 e^{-\delta n_m} n_m \delta^{-\frac{1}{2}} + 8\rho^4\left(e^{-\delta n_m}-1\right)\delta^{-\frac{1}{2}} \sim \delta^{-\frac{1}{2}} \quad (22)$$

As we can see, the characteristic relation ⟨n⟩∝$\epsilon^{-1/2}$

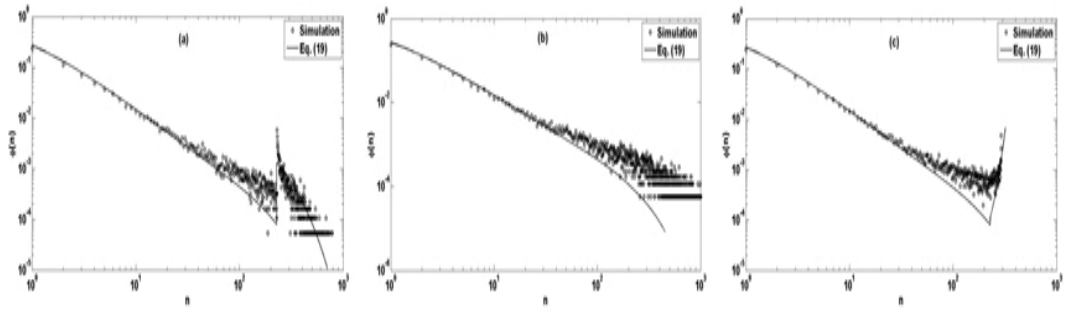

Figure 6. Logarithmic plots of the duration probability density φ(n) of interactions between reinjections for equation (2) with $\epsilon=10^{-2}$ and the trajectory of length $N=10^6$ based on different η: (a) η=6,(b) η=η_δ, and (c) η=6.5. The lines are theoretical predictions based on equation (19) with different approximation coefficients: (a) $r=2^3$, (b) $r=2^{-1}$, and (c) $r=2^{-8}e^{\wedge\epsilon 2n2}$.

As it can be seen in **Figure 6**, the starting curves of the duration probability density φ(n) are similar together as a clear exponential decay but at the end of the curves are different. For η>η_δ, it is as a classical asymmetrical U-shaped curve and for η=η_δ, it is as a clear exponential decay, but, the lower bound of the reinjection(x_l) affects it as an asymptotic mode in its curve for η<η_δ. Also, the approximation coefficient of equation (18) is independent of the number of interactions between reinjections for η ≤ η_δ but it depends on the number of interactions between reinjections for η>η_δ.

Now, if the reinjection value is considered in the vicinity of the fixed point, i.e. to consider |x|∈[0,τ] with τ~$\epsilon^{1/2}$, we can obtain the duration probability density of the laminar zone φ(l) using equation φ(l)=2 ψ(X(l))|(dX(l))/dl|. To consider |x|∈ [0, $\epsilon^{1/2}$], the reinjection probability density (RPD) ψ(X) is uniform and is equal to$\epsilon^{-1/2}$. In result, the duration probability density of the laminar zone φ(l) is as

$$\varphi(l) = \frac{\delta}{a}\frac{2e^{2\delta l}\left(\rho e^{2\delta l}-1\right)^{-\frac{3}{2}}}{\sqrt{1-\delta\left(\rho e^{2\delta l}-1\right)^{-1}}} \quad (23)$$

Here, we can again approximate the behavior of the duration probability density of the laminar zone φ(l) based on a characteristic laminar length scale l_m [34]. Therefore, we obtain for equation (23) an approximation as

$$\varphi(l) \approx \begin{cases} 6\left(l^2+8l+0.2\right)^{-1} & , l \ll l_m \\ 4\delta e^{-\delta l}, & l \gg l_m \end{cases} \quad (24)$$

If the upper bound for the local regular τ tends to δ, we can obtain numbers of interactions between reinjections (n) from the length of laminar zones (l), i.e. $\lim_{\tau\to\delta} l = n$. We can compute the characteristic relation of the average length of laminar zone ⟨l⟩ based on the above equation and ⟨l⟩=$l = \int_{l_0}^{\infty} l\varphi(l)dl,\ l_0 \cong 0$ [34]. We obtain the average length of laminar zone ⟨l⟩ as:

$$l \approx 6\int_{l_0}^{l_m} l\left(l^2+8l+0.2\right)^{-1}dl + 4\delta\int_{l_m}^{\infty} l\,e^{-\delta l}dl = 6.02\ln\left(5l_m+39.87\right)+22.19+4e^{-\delta l_m}l_m+4\left(e^{-\delta l_m}-1\right)\delta^{-1} \sim \delta^{-1} \quad (25)$$

The characteristic relation ⟨l⟩ of laminar zone is proportional to ϵ^{-1}.

THE BINARY BLOCK DESIGN

In this section, in order to optimize the Markov binary visibility graph to analyze the behavior of the dynamical system between reinjections in the type-III intermittency, we illustrate the binary block design. The block designs are topics in combinatorial mathematics which can be applied in all or part of methods and or algorithms of science classification in order to raise assortments of various phenomena in applied sciences [22,23]. In other words, a block design is the method of experimental design with η assigned treatments for a set of experimental units with z members in b blocks. The set of block sizes of τ is defined by $\{u_{\omega i}\}_{1<i<b}$

and the set of replications of treatments in τ are defined by $\{\zeta_{\omega i}\}_{1\le i\le \eta}$. If members of the set $\{u_{\omega i}\}_{1\le i\le b}$ and the set $\{\zeta_{\omega i}\}_{1<i<b}$ are equal to constant values υ and δ, respectively, then the design τ is called proper and equireplicate design. The incidence matrix $Z_\omega=[z_{\omega li}]$ is the characteristic function of the block design d where the z_{dli} is the number of iterates the *lth* treatment appears in the ith block [35]. A block design is binary if all of arrays Z_ω are equal to 0 or 1 [35]. In another word, if each treatment occurs at most once, in a block, the design is a Binary Block Design (BBD) [36]. The BBD is one of the versatile tools in pure and Applied Sciences [37-39].

TYPE-III INTERMITTENCY VERSUS MARKOV BINARY BLOCK VISIBILITY GRAPH

We first illustrate the Markov Binary Visibility Graph (MBVG) in which previous works was introduced [19,20]. The MBVG is a method to analyze fluctuations of a dynamical system. In fact, the MBVG maps the time series into a complex network based the Markov chain. A Markov chain is a discrete time process for which the future behavior and only depends on the present which has a set of states and transition probabilities between the states [20]. The set of the states plays an important role to analyze fluctuations in a dynamical system. Since the fluctuations between reinjections in type-III intermittency are slight during the transition of the dynamical system, the set of states in the Markov chain should be proportional to the slight fluctuations. One of the effective methods is the BBD which can design sets of the states so that the complex network proportional with them can inherit much more information from the slight fluctuations between reinjections. Here, we use a BBD within the structure of the MBVG with $b=z$ blocks that $\upsilon=\varsigma=1$ and $\eta=2$ treatments and hence rename the MBVG to Markov Binary Block Visibility Graph (MBBVG). To illustrate the structure the MBBVG, we first simulate the type-III intermittency based on time series $\{y_i\}_{1\le i\le z}$ of the equation (2) with $\epsilon=10^{-2}$. Then, we divide interval of the $\{y_i\}_{1\le i\le z}$ of the equation (2) to 2^μ areas which the μ is a rounded number to lower integer of logarithm of the infimum for time series $\{y_i\}_{1\le i\le z}$ of the equation (2), that is

$$\mu=-\log_2\left(\inf_{1\le i\le z} y_i\right) \tag{26}$$

where value of the μ is smaller or equal to 17. Therefore, the conditions of treatments can be considered as follows:

$$z_{\omega 1i}=\begin{cases}1 & \dfrac{2a-1}{2^\mu}\le y_i\le\dfrac{2a}{2^\mu}\\ 0 & otherwise\end{cases}, \tag{27}$$

And,

$$z_{\omega 2i}=\begin{cases}1 & \dfrac{2a-2}{2^\mu}\le y_i\le\dfrac{2a-1}{2^\mu}\\ 0 & otherwise\end{cases}, \tag{28}$$

where the a is equal to 1,2,...,2^μ. In result, we have an incidence matrix $Z_\tau=[z_{\omega li}]$ of the BBD with 2 rows and z columns. The incidence matrix inherits the more characteristics of fluctuations from the time series. In other words, the $z_{\omega 1i}$ and $z_{\omega 2i}$ are representatives of even and odd areas in the intermittent time series, respectively. Here, we use of the second row of the incidence matrix ($Z_{\omega 2}=[z_{\omega 2i}]_{i=1,...,n}$) as a set of states of Markov chain which is more appropriate for analyzing the type-III intermittency. Therefore, we have a Markov binary block sequence or a two-state Markov chain of Z_d2i bits which inherited the fluctuated behaviors of type-III intermittency from the time series. In the MBBVG, each bit of the Markov binary block sequence assigns to a node in the graph. Two nodes 'i' and 'j' in the MBBVG are connected, it can be draw a visibility line in the binary sequence joining the neighboring $z_{\omega 2i}$ and $z_{\omega 2j}$ that does not intersect any intermediate bits height [19]. Therefore, the *i* and the *j* are two connected nodes if the successive geometrical criterion is satisfied within the binary sequence as follows [20]:

$$z_{\omega 2i}+z_{\omega 2j}>z_{\omega 2h}\ \ that\ z_{\omega 2h}=0\ \ for\ \ i<h<j \tag{29}$$

Therefore, we have a graph similar to the MBVG which is always connected, undirected and the combination of two linear and maximal planar subgraphs [20]. As we know, in the MBVG, if the observer bit was bit 0, it may not observe some bits 0 (non visible bits) in the Markov binary sequence [20]. The MBBVG extracted from the time series of the equation (2) with $\epsilon=10^{-2}$ has the statistical (topological) properties which can analyze the behavior of dynamical system between reinjections in type-III intermittency. The Markov binary block sequence is characterized by transition probabilities P_(i→j) between the states {0,1}. The transition probability matrix P_{MBBS} of the Markov binary block sequence $Z_{\omega 2}$ is defined based on transition probabilities $P_{i\to j}$ as follows [20]:

$$P_{MBBS}=\begin{pmatrix}P_{1\to 1} & P_{1\to 0}\\ P_{0\to 1} & P_{0\to 0}\end{pmatrix}=\begin{pmatrix}P_1 & (1-P_1)\\ P_1 & (1-P_1)\end{pmatrix} \tag{30}$$

that P_1 and $(1-P_1)$ are the probability of bits of 1 and the probability of bits of zero in the Markov binary block sequence,

respectively. Here, for each k in the time series of the visibility degree there is a maximum of *k-1* different possible configurations $\{F_v\}_{v=0,\ldots,k-2}$ in the Markov binary block sequence $Z_{\omega 2}$ (see, for instance, [20]). The degree distribution *P(k)* is equal to the sum of associated probabilities of possible configurations $d(F_v)P(F_v)$ for degree of k and can be defined as follows:

$$P(k)=\sum_{v=0}^{k-2} d(F_v)P(F_v) \tag{31}$$

where $P(F_v)$ is the probability density function for each of the possible configurations. For, $k \geq 2$, the sum of the degree distribution is equal to 1, i.e. $\sum_{k\geq 2} P(k)=1$ [20]. The possible configurations distribution $P(F_v)$ or the joint probabilities distribution of the Markov binary block sequence $\{z_{\omega 2h}\}_{h=1,\ldots,m}$ corresponds to configuration F_v is obtained as follows

$$P(F_v)=\prod_{h=1}^{m}(P_{MBBS})_h$$

In result, we have the degree distribution as following

$$P(k)=d(k)\sum_{v=0}^{k-2}\left(\prod_{h=1}^{m}(P_{MBBS})_h\right) \tag{32}$$

That the *d(k)* is the probability density function for degree of k. Because of the structure of degrees time series extracted from the intermittent time series, degree distributions P(k) of them is similar to degree distributions in [20] with the difference that Markov binary sequence in MBV graphs give its place to Markov binary block sequence in MBBV graphs. In result, we can use theoretical degree distribution of [20] in order to predict experimental degree distribution of the MBBVG derived from the intermittent time series of type-III intermittency. Here, P_1 and $(1\text{-}P_1)$ are the probability of bits of 1 and the probability of bits of 0 in the Markov binary block sequence generated by the intermittent time series. According to the previous work [20], the degree distribution for chaotic and stochastic systems was defined in as follows

$$P(k)=(k-1)d(k)P_1(1-P_1)^{k-2}F(P_1) \tag{33}$$

Where

$$F(P_1)=\begin{cases}P_1 & k=2\\ P_1^2-P_1+1 & k=3\\ \frac{5}{3}P_1^2-\frac{5}{3}P_1+1 & k=4\\ P_1^2 & k\geq 5\end{cases} \tag{34}$$

As we know, if members of system be statistically dependent, the probability density function *d(k)* is equal to 1 unless value of degree k is more than or equal to 5 [20]. For, $k \geq 5$, the ϵ and also standard deviation σ of the Markov binary block sequence derived from the intermittent time series of type-III intermittency can affect the probability density function *d(k)*. Because of independent of the non-laminar zones from channel widths, the probability density function *d(k)* is equal to 1 [20]. We plot in logarithmic diagrams the experimental and theoretical degree distributions of the Markov binary block sequence derived from the intermittent time series of type-III intermittency **(Figure 7)**.

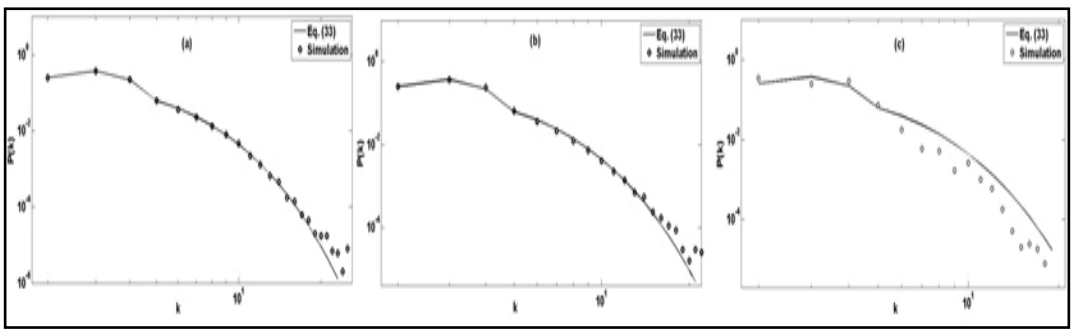

Figure 7. Three log-log plots of degree distributions of MBBV graphs extracted from the intermittent time series of the equation (4) with $\epsilon=10^{-2}$ and the trajectory of length $N=10^6$ based on different η: (a) η=6,(b) $\eta=\eta_\delta$, and (c) η=6.5. Solid lines P(k) correspond to equation (33).

Numerical results show which the experimental degree distribution of the MBBVG derived from the intermittent time series can be predicted by equation (33) and also equation (33) can distinguish two states $\eta \leq \eta_\delta$ and $\eta>\eta_\delta$ from each other in type-III intermittency. Finally, results show the MBBV graph can analyze the fluctuated properties of the intermittent time series in type-III intermittency based on degree distributions which are in agreement with previous results [30,34].

CONCLUSION

In this work, we have investigated the effect of the asymptotic mode and new nonlinear term on the behavior of type-III intermittency using the function of sin(x). Results showed that the length of laminar is proportional to the behavior of the asymptotic mode and new nonlinear term in the interval [-δ,δ]. We have obtained the average number of iterations as characteristic relations $\langle n \rangle \propto \epsilon^{-1/2}$ type-III intermittency. Also, the average of the laminar zone has been computed and the results showed the average of the laminar zone is approximately proportional to ϵ^{-1}. Finally, we used the binary block design in the MBV algorithm for introducing the MBBV graph in order to optimize it to better analyze the type-III intermittency. The complex network perspective of the MBBV graph illustrates some fluctuated properties of iterations between reinjection points in intermittency type-III, that is, it can distinguish two states $\eta \leq \eta_\delta$ and $\eta > \eta_\delta$ from each other in type-III intermittency. This work again confirmed the capability of the MBV graphs for analyzing the various types of complex systems.

ACKNOWLEDGMENT

We would like to thank Yaser Sadra for many helpful discussions.

REFERENCES

1. Manneville P, et al. Intermittency and the Lorenz model. Phys Lett A. 1979;75:1-2.
2. Sergio E, et al. Studies for type-I, type-II and type-III intermittencies. Mecánica Computacional. 2010; 29:3389-3406.
3. Price T, et al. An experimental observation of a new type of intermittency. Phys D. 1991;48:29-52.
4. Bauer M, et al. New type of intermittency in discontinuous maps. Phys Rev Lett. 1992;68:1625-1628.
5. He D, et al. Type V intermittency. Phys Lett A. 1992;171:61-65
6. Fan J, et al. The distribution of laminar lengths in type V intermittency. Phys Lett A. 1993;182:232-237.
7. Platt N, et al. On-off intermittency: a mechanism for bursting. Phys Rev Lett. 1993;70:279-282.
8. Heagy J, et al. Characterization of on-off intermittency. Phys Rev E. 1994;49:1140-1150.
9. Pikovsky A, et al. Attractor-repeller collision and eyelet intermittency at the transition to phase synchronization. Phys Rev Lett. 1997;79:47-50.
10. Kurovskaya M. Distribution of laminar phases at eyelet-type intermittency. Tech Phys Lett. 2008;34:1063-1065.
11. S Elaskar, et al. New Advances on Chaotic Intermittency and its Applications, Springer. 2017;35-38.
12. Hramov AE, et al. Ring intermittency in coupled chaotic oscillators at the boundary of phase synchronization. Phys Rev Lett. 2006;97:114101.
13. Kim CM, et al. New characteristic relations in Type-I intermittency. Phys Rev Lett. 1994;73:525-528.
14. Hugo LD, et al. Averages and critical exponents in type-III intermittent chaos. Phys Rev E. 2002;026210.
15. Fukushima K, et al. Type-III Intermittency in a coupled nonlinear LCR circuit. J Phys Soc Japan. 1988;57:4055.
16. Ono Y, et al. Critical behavior for the onset of type-III intermittency observed in an electronic circuit. Phys Rev E. 1995;52:4520.
17. Tang DY, et al. Type-III intermittency of a laser. Phys Rev A. 1991;44:R35.
18. Griffith TM, et al. Critical scaling and type-III intermittent chaos in isolated rabbit resistance arteries. Phys Rev E. 1997;56:R6287.
19. Ahadpour S, et al. Randomness criteria in binary visibility graph and complex network perspective, Information Sciences. 2012;197:161-176.
20. Ahadpour S, et al. Markov-binary visibility graph: A new method for analyzing complex systems, Information Sciences. 2014;274:286-302.
21. Colbourn, et al. Handbook of combinatorial designs. Boca Raton: Chapman and Hall. 2007;17-19.
22. Stinson, et al. Combinatorial designs: Constructions and analysis. Springer, New York. 2003;1-3.
23. Earl SK. Finite geometries and combinatorial designs. Am Math Soc. 1990.
24. Dunietzl IS, et al. Applying design of experiments to software testing, Proceedings of the (19th) International Conference on Software Engineering. 1997:205-215.
25. Zhao G, et al. Block cipher design: Generalized single-use-algorithm based on chaos. Tsinghua Sci Technol. 2011;16:194-206.

26. Ahadpour S, et al. A novel chaotic encryption scheme based on pseudorandom bit padding. IJCSI Int J Comput Sci. 2012;9:449-456.
27. Hanzo L. Short block codes for guaranteed convergence in soft-bit assisted iterative joint source and channel decoding. Electronics Lett. 2008;44:1315-1316.
28. Dubois M, et al. Experimental evidence of intermittencies associated with a subharmonic bifurcation. Phys Rev Lett. 1983;51:1446.
29. Laugesen N, et al. Anomalous statistics for type-III intermittency. Open Syst Inf Dyn. 1997;4:393-405.
30. Elaskar S, et al. Reinjection probability density in type-III intermittency. Phys A. 2011;2759-2768.
31. Rio ED, et al. Effect of noise on the reinjection probability density in intermittency. Commun Nonlinear Sci Numer Simulat. 2012;17:3587-3596.
32. Elaskar S, et al. Reinjection probability function with lower bound of the reinjection for intermittency type III. Mecánica Computacional. 2009;28:1463-1475.
33. Del ER, et al. New characteristic relations in type-ii intermittency. Int J Bifurcation Chaos. 2010;20:1185-1191.
34. Nune AM, et al. Horizontal visibility graphs generated by type-II intermittency. J Phys A Math Theor. 2014;47.
35. Aloke D. Incomplete block designs, Hindustan Book Agency (HBA). 2010;6-7.
36. Rashid A, et al. Journal of Statistics. 2008;5:1-6.
37. Ghosh S, et al. Efficiency of connected binary block designs when a single observation is unavailable. Ann Inst Stat Math. 1992;44:593-603.
38. Godolphin JD, et al. An efficient procedure for the avoidance of disconnected incomplete block designs. Comput Stat Data Anal. 2014;71:1134-1146.
39. Godolphin JD, et al. The robustness of resolvable block designs against the loss of whole blocks or replicates. J Stat Plan Inference. 2015;163:34-42.